Research Article

Cost and duration estimation of autonomous grading algorithm by simulation

Önder Halis BETTEMIR[1],*

[1]Department of Civil Engineering, İnönü University, Malatya, 44280, Türkiye

ABSTRACT

Estimation of cost and duration of grading a particular area provides important information for contractors and construction machine manufacturers. In this study, cost and duration of excavation by dozer is estimated by simulating the movements of the dozer. Specifications of the dozer, soil conditions and site conditions are defined to the simulator. The simulation considers tire penetration, rolling, grade, hauling, as well as cutting resistances and estimates the necessary force to be applied. The simulation implements an autonomous grading algorithm established for electric powered dozers which starts grading from a local highest point to prevent uphill excavation and hauling. The algorithm determines the necessary maneuvers to reach local highest point, excavate or haul the earth pile to the dump area. The simulation runs until the objected elevation is obtained at each portion of the excavation site. The simulator calculates the consumed energy, time, and total cost of the excavation. The excavations of 30x45 square meter area by one existing electric dozer and five updated versions of it are simulated. The simulation of the excavation is computed in 23 seconds for the smallest and 10 seconds for the largest dozer. The cost of grading and pushing the excavated material at most 20 meters away is estimated as less than 5 cents/m3 for the lead-acid battery powered dozer and 8 cents/m3 in the average for the lithium-ion battery powered dozers. The simulation revealed that electric powered dozers have less unit excavation cost than diesel powered ones, also larger dozers consumes less energy than the smaller ones. The developed simulation technique is implemented without any numerical errors and the technique can be beneficial for the construction machine manufacturers to optimize their designs and for the contractors to select the most suitable construction machine among the present alternatives.

Cite this article as: Bettemir ÖH. Cost and duration estimation of autonomous grading algorithm by simulation. Sigma J Eng Nat Sci 2024;42(3):831–844.

INTRODUCTION

Earthwork tasks are executed at outside which may cause execution of them under severe weather conditions. The construction machines must be operated very carefully in order to avoid occupational accident. Long working time and severe weather conditions may decrease the efficiency of the operator and cause distractibility. Utilization

*Corresponding author.
*E-mail address: onder.bettemir@inonu.edu.tr

of construction machines requires significant amount of investment, consequently, the contractors aim to obtain the highest efficiency and safety. To increase the output of the construction machines, numerous works are conducted on the machine control and automation. Discounts in Continuously Operating Reference Station Global Positioning System (CORS GPS) receivers, gyroscopes and accelerometers, as well as computers made the machine control and automation systems affordable for the construction machines.

The theoretical studies increased the efficiency of the machine control systems. Zong et al. analyzed the earth fill dam construction process by defining the coordinates of the compaction machines according to the construction plan [1]. Lu et al. obtained the position of the construction machines by GPS receivers and inertial navigation systems. The system executes the data transfer among the construction machines by a Bluetooth system to avoid collision [2]. Vahdatikhaki et al. estimated the position and orientation of the excavator and cranes with real time location systems. In the analysis, 27 cm positional and 12" orientation accuracies are obtained within 90% confidence interval [3]. Hammad et al. simulated earthwork operations by 1/24 scale radio controlled truck and 1/12 scale radio controlled excavator. The location and the movements of the excavator and the truck is measured and recorded by ultra-wideband locating and tracking technique. Duration of four full cycles including the loading, hauling, dumping, and return operations are estimated as 267 seconds by simulation but the real application is completed in 280 seconds [4].

Jurasz and Kley developed a machine control system with a low cost GPS receiver for the asphalt rollers. The developed system improves the construction quality and decrease the cost of the highway constructions [5]. Hung and Kang developed an autonomous clustering algorithm to detect collisions. The algorithm is an iterative method which is based on k-means clustering algorithm to decrease the computational demand of the construction simulation [6]. Oloufa et al. developed an equipment tracking and collision detection system based on GPS positioning and wireless communication technology. The system warns the operators of the construction machines if the system perceives a probable collision by considering the velocities and the positions of the construction machines [7, 8].

Hammad et al. conducted three case studies to detect the collision of tower cranes, to simulate hauling trucks, and to detect conflicts of a bridge construction. The case studies revealed that 3D modeling and real-time visualization models increase the productivity and efficiency [9]. ElNimr et al. implemented discrete event simulation to model the movements and maneuvers of mobile cranes. The ongoing construction activities and the relocation of the corresponding temporary facilities are simulated. A mesh is generated to represent the construction site and motions of the cranes are modeled by A* algorithm. The

schedule and resource availabilities are analyzed and the construction process is visualized [10].

Vahdatikhaki and Hammad developed a near-real time simulation system to assess occupational safety of the construction site. The algorithm implements a parametric motion planning algorithm and predicts the motion of the construction machines. If a possible collision is detected, the path of the construction machines are altered [11]. Autonomous machines and machine control systems have important applications on the agriculture and farming. Blackmore and Griepentrog investigated the capabilities of the driver assistance including the crop edge detection, self-guiding inter-row weeder, and autonomous tractors [12]. Murad and Yıldız listed possible autonomous farm-machine applications at the greenhouses. The pesticide spraying, copping of plants, and harvesting are the main examples of the research [13]. Kılıç and Kapucu developed and manufactured a multi-purpose and reconfigurable autonomous robot [14]. Bettemir and Tombaloğlu designed and developed an autonomous grader for the earthwork tasks [15]. Yıldırım and Bettemir implemented a grading algorithm for the autonomous grading task. The algorithm is proposed for electric powered graders which have low rimpull [16]. Bettemir simulated the positional and angular accuracies of D-GPS receivers assembled on an autonomous machine and performed cost estimation of the design [17, 18].

Design of a dozer requires the prediction of the resistive forces during the excavation and hauling of the earth. Fall et al. estimated the deviation of the frictional coefficient of the sand with respect to moisture content. The analysis concluded that the frictional coefficient decreases if the moisture content of the dry sand is increased until it reaches the optimum ratio [19]. Klanfar et al. estimated the output of a dozer on open pits by considering the engine power and the resistive forces on the dozer. Photogrammetric measurements are conducted in order to estimate the capacity of the dozer blade [20]. Pattel et al. analytically estimated and compared the resistive forces of the excavation task by McKyes and Zeng models [21-23]. Even though the compared models have different analytical expressions, their output is close for the average soil parameters. Xia developed a combined analytical and numerical method for the estimation of the resistive forces on the dozer blade. The model enables changes in the raw, pitch, and yaw angles of the dozer blade [24]. The volume of the spilled earth is computed iteratively which changes according to the height of the hauled earth and the grading angle of the dozer. The developed model is tested on the TOMSIM and DYNASTY modules of Caterpillar.

The aforementioned resistive force estimation algorithms have sufficient accuracy when the variability of the in situ soil condition is considered. On the other hand, the existing simulation models cannot autonomously generate maneuvers, a human operates the simulator and the resultant energy consumption and excavation duration is

computed. The state of the art machine control systems are not autonomous and they depend on the commands of the operator. On the other hand, the near future space missions aim to setup colonies on the Moon and Mars where the distance is too long which makes remote control impractical. This study aims to contribute the literature by generating a force model for the autonomous grading algorithm and compute the cost and duration of the excavation by dozer. In this study, autonomous grading of a land is simulated and the resistive forces on the dozer blade and the dozer are predicted simultaneously. The sufficiency of the rimpull is ensured by adjusting the depth of cut and the volume of the pushed excavated material by the blade. The consumed energy is estimated by considering the applied rimpull. The obtained results are used to examine the capability of the dozer and the cost and duration of the grading task. The simulation software is generated on C++ in order to execute the computations. The rest of the manuscript briefly introduces the developed dozer, the autonomous grading algorithm, and the simulation process. Then the case study where the developed algorithms are tested is introduced and finally the results are discussed and concluded.

METHODOLOGY

In this section the unmanned dozer, the autonomous grading algorithm, forces on the dozer, and the simulation process is briefly introduced.

Unmanned Dozer

This study is based on the autonomous small scale grader which is designed and manufactured by the 110M396 grant of the scientific and technological research council of Türkiye. The small scale dozer shown in Figure 1 and 2 has 1.25 meters of blade width and powered by four electric motors for motion and six electric motors for the blade maneuver. The small scale dozer is can grade soft soils.

In Figure 1, electric motors represented as 1 and 2 work in pairs and supply the vertical movement. If the electric motors 3 and 4 push the blade forward and electric blades 5 and 6 pull the blade backwards, the blade rotates horizontally in clockwise direction. The reverse movement rotates the dozer blade in counter-clockwise direction. If the electric motors 3 and 5 pull the blade and electric motors 4 and
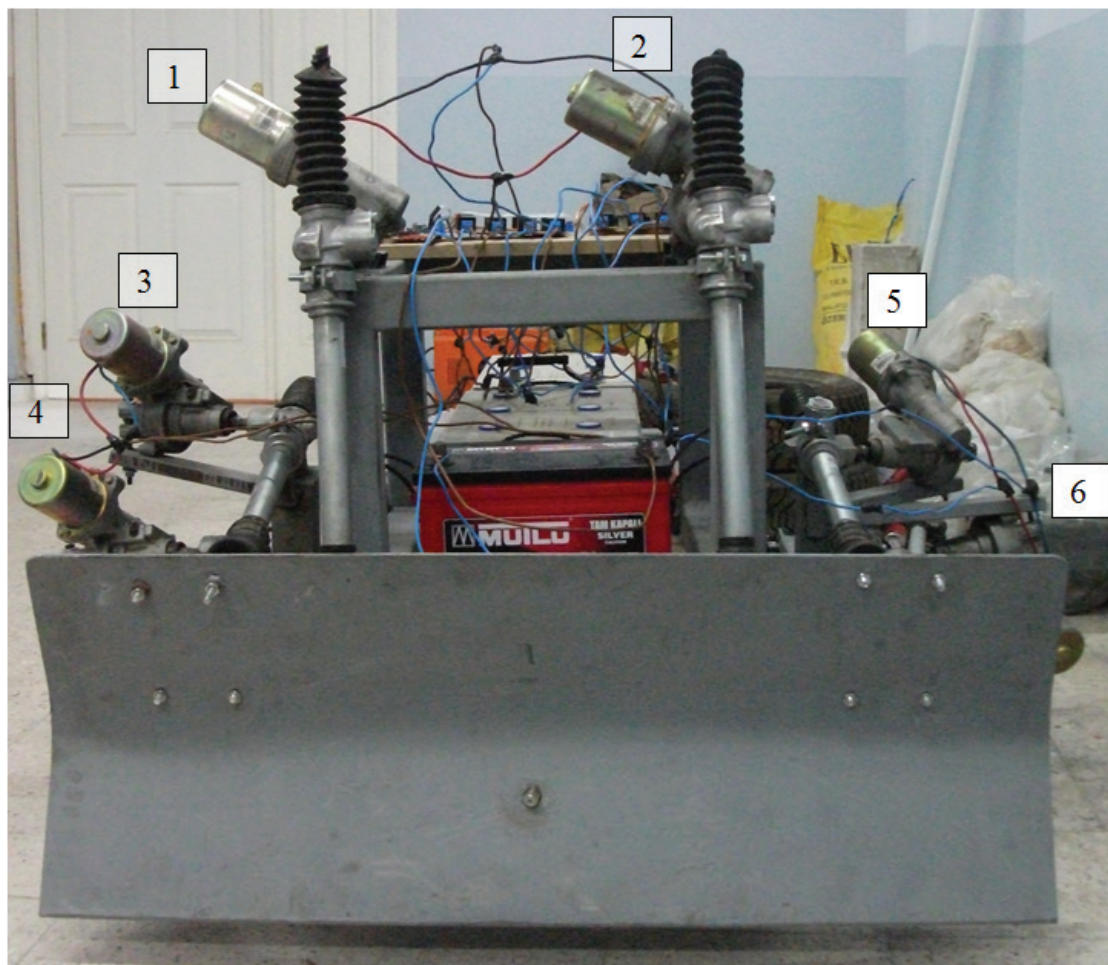

Figure 1. Position of the six electric motors for the movement of the dozer blade.

Figure 2. The ready to operate state of the small scale dozer.

6 push the blade, the rake angle increases. If the movement of the electric motors is reversed the rake angle decreases.

In Figure 2, the ready to operate state of the dozer is shown. The lead dioxide accumulators provide the electric power to the motors. The red lead dioxide accumulator supplies power to the GPS receiver and the motor control circuits. The assembled laptop computer has its own power supply.

In Figure 3 dimensions of the some of the components of the dozer is represented in cm. Design and production of the autonomous dozer is realized with a small budget, therefore the capacity of the accumulators and the rimpull force of the traction motors are limited. In this study, unit excavation costs of more expensive design configurations with more powerful electric motors and lithium-ion batteries are also examined.

Autonomous Grading Algorithm

Traction force of the electric motor powered dozer is less than the diesel engine powered dozers. Therefore, a special autonomous grading algorithm is proposed for the electric powered dozers. The proposed method prevents uphill grading and transportation of the excavated earth pile by commencing the excavation task from the local maximum elevation. The grading algorithm increases the
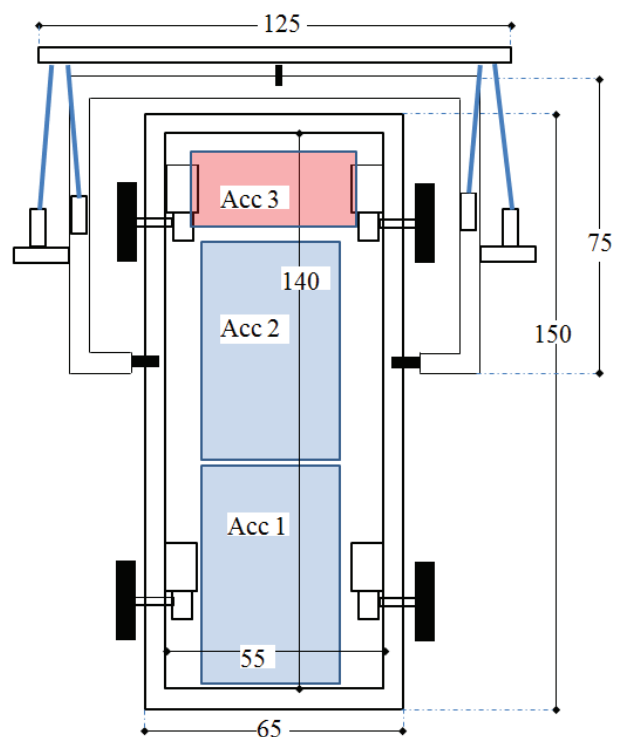

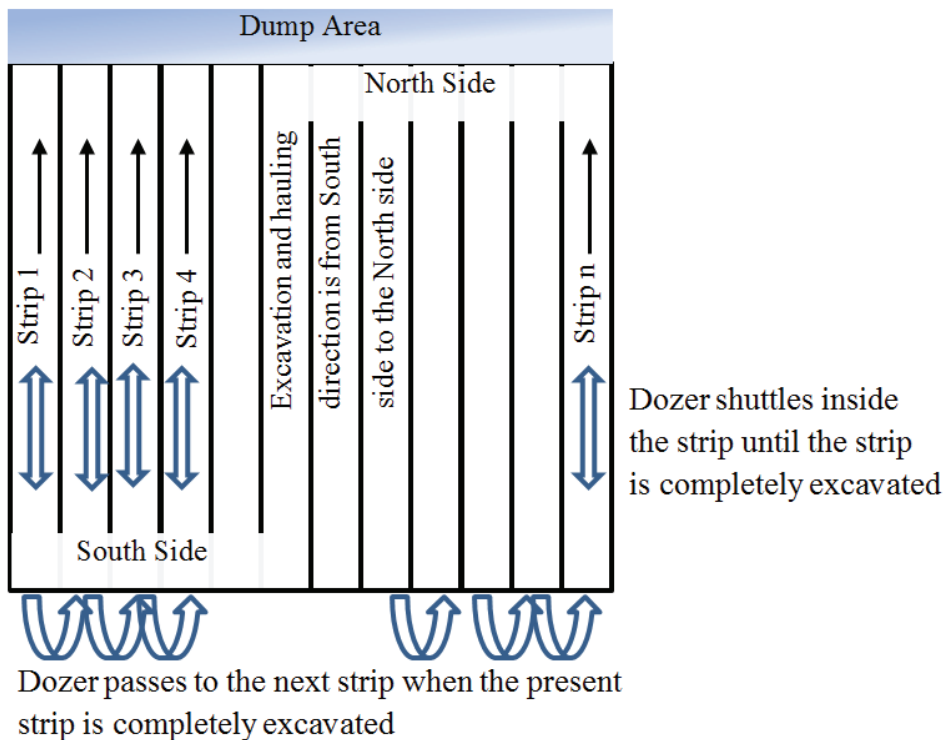**Figure 3.** Dimensions of the dozer.

Figure 4. Representation of the grading strips of the excavation zone.

duration of excavation because it elongates the path of the dozer in order to prevent uphill grading. The excavation is executed strip by strip as shown in Figure 4.

Width of the dozer blade is assigned for the widths of the strips. The number of strips is equal to the width of the excavation zone divided by the width of the dozer blade. The dozer shuttles inside the strip until the required ground elevation is obtained. Then the dozer passes to the next strip. The grading algorithm is represented by the following pseudo-code.

Start
> ***Go*** *to the front side of the strip*
> ***Find*** *the nearest local highest point*
> ***Go*** *to the nearest local highest point*
> ***Start*** *excavating the local highest point*
> ***Excavate***
> > ***if*** *the ground level is higher than the red line*
> ***Stop excavating***
> > ***if*** *the earth pile reaches the blade capacity*
> > > ***Push*** *the excavated earth to the dump area*
> ***Unload*** *the dozer blade when it arrives at the dump area*
> ***Update*** *the ground elevation model*
> ***Find*** *the nearest local highest point*
> ***Repeat*** *all of the steps until the desired elevation is obtained*

Go *to the next strip*
End If *all of the strips are graded*

The aforementioned grading algorithm is programmed in C++ without analyzing the forces and it is shown that it can successfully grade the predefined excavation area [16]. The grading sequences of the algorithm are visualized without computing any forces on the construction machine [25].

Calculation of the Resistive Forces

The resistive forces acting on the dozer during the grading can be listed as; rolling, tire penetration, grade, cutting, and hauling resistances as shown in Figure 5.

Rolling resistance

Tire of the construction machine deflects due to the exerted forces on the tire. The shape of the tire is deflected continuously which causes energy loss as it rolls. The mentioned energy loss is classified as rolling resistance and its value for radial tires is suggested as 20 kg/ton [26].

Tire penetration resistance

Tire penetration resistance occurs when the ground surface has low load bearing capacity. Tires penetrate into the ground and as the construction machine moves forward the tires proceed by splitting the soil. The force applied to deform the ground surface is called the tire penetration resistance. This resistance is correlated with the depth of the penetration and it is calculated by Eq. 1 [26].
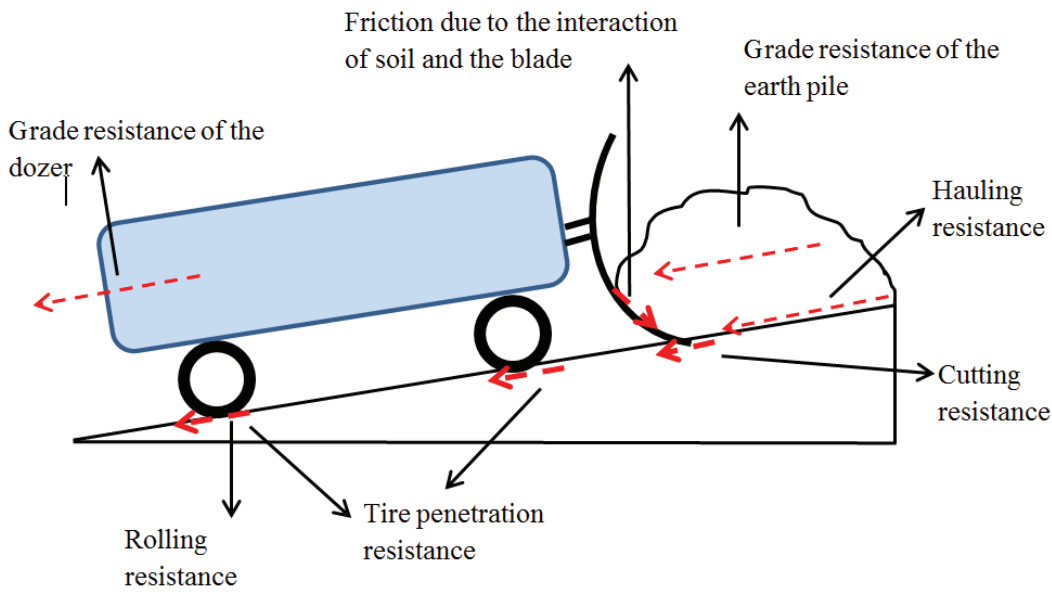
$$PR = 6 * P \tag{1}$$

Figure 5. Illustration of the resistive forces that occur during the grading task.

Where PR is the penetration resistance in kg/ton, P is the depth of penetration in cm and 6 is a coefficient related with the toughness of the surface and it is in kg/ton/cm [26].

Grade resistance

Grade resistance occurs when the dozers moves uphill. Unit of the aforementioned resistance is taken as kg in order to facilitate perception. Each %1 uphill slope ends up with 10 kg of resistance per ton of the dozer. Grade resistance assists the dozer to outstrip the remaining forces acting on the dozer, if the machine moves downhill. Grade resistive force is illustrated in Eq. 2.

$$GR = 10 * s * [m_d + m_e] \tag{2}$$

where, s is the slope of the ground represented as percent. If the dozer moves downhill s becomes negative, m_d represents the mass of the dozer, m_e illustrates the mass of the excavated earth material pushed by the blade of the dozer, and GR is the grade resistance.

Hauling resistance

The excavated material being pushed on the earth surface is exposed to frictional force because of the interaction between the ground surface and the excavated particles. The hauling resistance, HR is illustrated in Eq. 3 [20].

$$HR = \gamma_l V \left(\mu + \tan \delta * \cos^2 \alpha \right) \tag{3}$$

In Eq. 3 γ_l represents the loose density, V is the volume of the transported earth by the dozer blade, μ is the coefficient of friction among the hauled earth in front of the blade and the earth surface, δ is the coefficient of friction

between the hauled earth and the blade of the dozer, α is the penetration angle of the dozer blade when it excavates the earth surface.

Cutting resistance

The excavated soil resists the dozer blade at its passive state. The dozer moves forward with its blade penetrating the ground which causes the soil particles in front of the blade to compress. The aforementioned compression is the cause of the passive force. The penetration angle, internal friction angle of the soil, and slope affects the required force to exert to achieve cutting as represented in Eq. 4 [27].

$$CR = \left(\gamma g d^2 N_\gamma + cd N_c + q d N_q + c_a d N_a \right) w \tag{4}$$

In Eq. 4, where

$$N_\gamma = \frac{(\cot\alpha + \cot\beta)\sin(s + \phi + \beta)}{2\sin(\delta + \alpha + \phi + \beta)}$$

$$N_c = \frac{\cos(\phi)}{\sin(\beta)\sin(\delta + \alpha + \phi + \beta)}$$

$$N_q = \frac{\sin(s + \phi + \beta)}{\sin(\delta + \alpha + \phi + \beta)}$$

$$N_a = \frac{-\cos(\alpha + \phi + \beta)}{\sin(\alpha)\sin(\delta + \alpha + \phi + \beta)}$$

In the set of equations soil cohesion is represented by c with N/m², d represents the depth of penetration of dozer blade into soil in m, γ represents the natural density of the soil in N/m³, surcharge pressure is represented by q in N/m², coefficient of adhesion between the soil and the metal blade of the dozer is represented by c_a in N/m², angle of internal shearing resistance is represented by ϕ, δ is the angle of soil to metal friction, β is the angle of rupture, s is the slope of the topography where the dozer works, and angle between the dozer blade and the soil is represented by α. Angle of rupture is affected by α, ϕ, and δ coefficients

and it is not constant through the grading process. Reece suggests computation of angle of rupture as a minimization process of N_γ [28, 29]. In this study in order to detect the minimum of N_γ complete evaluation procedure is implemented by assigning values 0^0 to 90^0 to β with increments of 1^0 and the obtained minimum value of N_γ is utilized [21].

The parameter c_a has important effect on the output of the dozer since it is the coefficient of adhesion due to the interaction between the soil and the dozer blade. The studies to reduce the friction and the wear aim to improve the efficiency of the construction machine. Frictional coefficient of the metal surface can be decreased when soft metal coating is utilized. This can improve the soil blade interaction because humid air or water may provide formation of silicon oxide or silicon hydro-oxide subjected to frequent rolling contact or collision of soil particles. The mentioned oxides or hydro-oxides are soft or soluble in humid air or water. This makes the wear surfaces suitable for hydro-dynamic lubrication obtained by water. For this reason, a reaction layer on a firm ceramic layer performs as a soft covering [30]. Hard chrome, PVD CrN and Cr conversion coatings are usually utilized to enhance the mechanical properties against the corrosion and wear of the components [31]. It is difficult to distribute nano-sized reinforcing elements in the matrix. In addition to this, obtaining economic filler which maintains the homogeneity of the composite is the second problem [32]. Metal matrix syntactic foams (MMSF) have high energy absorption capacity so that it can reduce the weight of the construction machine and provide high impact resistance. Pumice elements utilized to cover space in the AA7075 matrix to produce MMSF and enhancements in the average compressive strength are obtained. The mentioned properties deteriorate when the particle size of the filler increases [33]. The Finite Element Model reveals that the TiB_2 and AlN coated samples provide the highest strength which is valid for different temperatures [34].

Simulation Process

The simulation process requires the digital elevation model (DEM) of the land, soil conditions, and technical qualifications of the construction machine as input data. The grading is simulated as strips which are represented in Figure 4. The simulation process is executed by dividing the construction area into square meshes, whose size is equal to the width of the dozer blade in order to update the elevation of the excavated portion consistently. However, the spatial resolution of the DEM and the mesh size may not overlap. In this case, the elevation of the mesh is estimated by the resampling process illustrated in Figure 6 by bilinear interpolation technique given in Eq. 5 [35].

$$P = \frac{(x_2 - x)(y_2 - y)}{(x_2 - x_1)(y_2 - y_1)}Q_{11} + \frac{(x - x_1)(y_2 - y)}{(x_2 - x_1)(y_2 - y_1)}Q_{21}$$
$$+ \frac{(x_2 - x)(y - y_1)}{(x_2 - x_1)(y_2 - y_1)}Q_{12} + \frac{(x - x_1)(y - y_1)}{(x_2 - x_1)(y_2 - y_1)}Q_{22} \tag{5}$$

In Eq. 5, Q_{ij} represents the elevation of the interpolation points in the DEM, x_i and y_i represents the coordinates of the ith interpolation point, and x and y are the coordinates of the estimation point, P is the estimated elevation of the estimation point. Eq. 5 is implemented for every point of the square meshes. Q_{ij} are the nearest four points to the estimation points. If the points on the DEM and the square mesh coincide then Eq. 5 is not implemented and the elevation of DEM is assigned to the corresponding point of the square mesh.

Interpolation introduces an error for the estimated grid heights. The error is proportional with the interpolation distance and the rate of change of the interpolated function. In image analysis the bilinear interpolation technique is widely implemented and successful results are obtained. A digital image would have more abrupt changes compared with the shape of a terrain. Shi et al. examined the error propagation of bilinear and higher order techniques
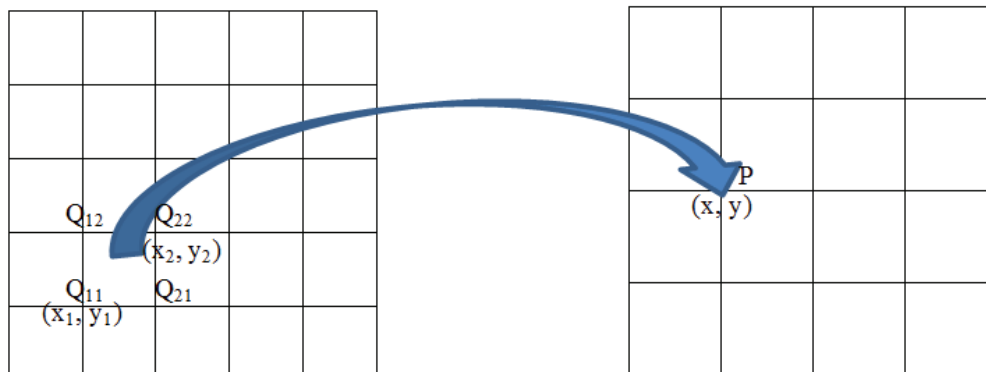

Figure 6. Illustration of resampling process of the digital elevation model.

and deduced that the error propagation is related with the $\sigma_H^2 = \frac{4}{9}c$ for all of the methods [36]. In the formula σ_H^2 is the variance of the elevation values of each node of the perpendicular grid network. In addition to this, the interpolation distance is very small which preserves the amplification of the error. The interpolation equations are linear therefore; the total volume of the excavation site is preserved.

The time interval of the simulation depends on the mesh size and the velocity of the dozer. The dozer can be at moving empty, excavating, and hauling states. The velocities of each state are different. The notion of time of the simulation process is determined as given in Eq. 6.

$$T_{i+1} = T_i + \Delta T_i \tag{6}$$

where $\Delta T_i = \frac{w}{v_i}$. Size of the mesh is equal to the width of the dozer blade, w, and v_i is the velocity of the dozer at the ith step of the simulation. Every physical, geometric and mechanical factor is assumed to be fixed during the steps of the simulation. The mesh size is equal to the blade width of the dozer which is at most 1.5 meters. The mentioned mesh size is small enough for the constant slope, cutting depth, acceleration, resistive forces and power consumption assumptions. The simulation parameters are recomputed and updated for each grid. This minimizes the accumulation of errors. The accuracy of the state of the art DEM generation techniques can provide at most 10 cm of theoretical accuracy for 300 m² x 300 m² area [37]. The deviation of the topography from the simulation model at the ith step is within ± 1cm range for rough terrain. This shows that the assumptions of the simulation contribute negligible errors when compared with the error of the DEM. The state of the machine is decided by considering the grading algorithm. Grader will move in empty state if its destination is the local highest point. The state of the grader is excavating if the grader has reached the highest local point, and the pushed earth pile is less than the blade capacity, and the elevation of the ground is higher than the red line. The state of the grader is hauling if the grader has reached the local highest point, and the pushed earth pile is equal to the blade capacity or the present elevation is equal to the elevation of the red line. The forces on the dozer are computed by implementing Eqs. 1 to 4. The soil parameters are assumed to be constant since the grading area is not large. The parameters which are subjected to change are the ground slope and the amount of the earth pile transported by the blade. The slope of the ground at the ith state of the simulation (s_i) is determined by Equation 7.

$$s_i = \frac{P_{i+1} - P_i}{w} \tag{7}$$

In Eq. 7 difference between the elevation of the next grid and the present grid is computed and it is divided by the width of the dozer blade. In order to make the simulation process easier, grid size is taken as equal to the width of the dozer blade. The volume of the excavated material hauled by the dozer is kept constant when the construction machine does not excavate. This assumption depends on the equivalence of the discharge of the hauled material from the edges of the dozer blade and the excavated soft soil because of the interaction of the dozer blade and the terrain. Amount of the excavated material transported by the blade of the dozer is represented in Eq. 8.

$$V_{i+1} = V_i + w * d_i * k_s \tag{8}$$

In Eq. 8 d_i represents the amount of the penetration of the dozer blade into the soil at the ith pace of the simulation. It becomes zero when the construction machine is not excavating. Swell factor of the excavated material is represented by k_s Amount of the hauled material is reset to zero when the construction machine arrives at the dump zone. Eq. 9 is implemented to update the elevation value of the mesh if it is excavated.

$$P(x, y)_{T_{i+1}} = P(x, y)_{T_i} - d_i \tag{9}$$

$P(x, y)_{T_i}$ is the elevation of the mesh point with coordinates (x, y) at the ith step of the simulation. Net resisting force acting on the construction machine is determined as given in Eq. 10.

$$F_i = \left[GR_i + RR + PR_i\right] * g + CR_i + HR_i + \left[m_d + m_e\right]_i a_i \tag{10}$$

In Eq. 10, RR represents the rolling resistance which is 20 kg/ton, g is the gravitational acceleration, a_i is the acceleration at the ith step of the simulation which is equal to $\frac{v_{i+1} - v_i}{\Delta T_i}$ and $\left[m_d + m_e\right]_i$ is the mass of the dozer including the earth pile at the ith step of the simulation. Acceleration is kept fixed throughout the ΔT_i time interval. The required force should be less than or equal to the m_d*f_t where m_d is the mass of the dozer and f_t is the frictional coefficient between the tires and the surface of the ground. The required power to deliver the essential traction force is calculated by Eq. 11.

$$PW_i = \frac{F_i * v_i}{\eta_m} \tag{11}$$

In Eq. 11 η_m is the efficiency of the electric motors, v_i is the velocity of the dozer. In case of steep downhill motion, F_i can be nonnegative. In such a case, F_i becomes zero. The required energy is calculated as given in Eq. 12.

$$CE_{i+1} = CE_i + PW_i * \Delta T_i \tag{12}$$

The simulation continues until the elevations of all of the strips are reduced to the design level. Finally the required energy is calculated by $CE = \frac{CE_T}{\eta_a}$ where T is the last step of the simulation and η_a is the efficiency of the accumulators.
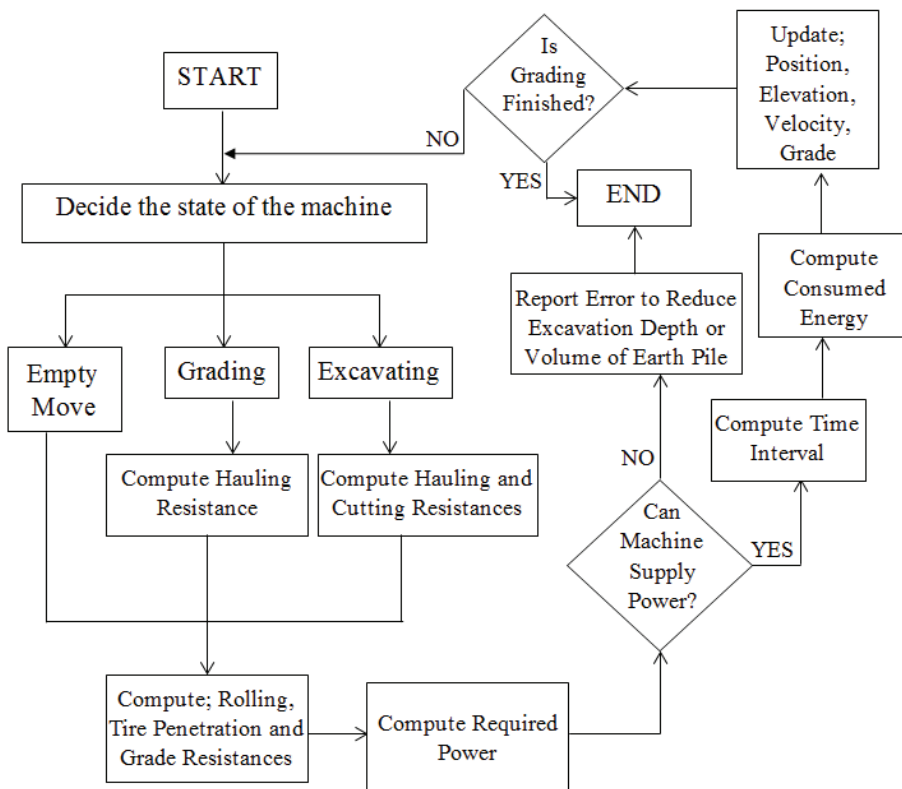
Figure 7. Flowchart of the simulation process.

The cost of the earthwork task is determined by considering the costs related with the construction machine and the energy costs. Fixed cost of the dozer is obtained by implementing the Eq. 13.

$$FixedCost = \frac{A}{Nn} + 0.53\frac{A}{Nn} + 0.13\frac{A}{Nn} + i\frac{A(N+1)}{2Nn} + 0.02\frac{A}{n} \quad (13)$$

In Eq. 13, A is the investment cost, N is the useful life, n is the number of hours that the machine works in a year, i is the ratio of capital cost of the construction machine. The terms are named as depreciation, spare parts, repair and maintenance, capital, dismantling and transportation costs respectively. According to the Republic of Türkiye Ministry of

Environment, Urbanization and Climate Change, N = 8 years, n = 2000 hours/year, i=8% for the construction machines.

The flowchart of the simulation process is illustrated in Figure 7.

CASE STUDY

The developed simulation algorithm is tested on the manufactured dozer D1, and five fictitious electric powered dozers whose specifications are illustrated in Table 1. The capacity of the present dozer illustrated in Figure 2 is low compared to the one used in real life thus more powerful dozers are also selected to simulate. The simulation aims to reveal the cost and duration of the earthwork executed by

Table 1. Mechanical specifications of the simulated dozers.

	D1	D2	D3	D4	D5	D6
Electric Motors (watt)	4x300	4x500	4x750	4x1000	4x1500	4x2500
Total Weight (kg)	450	400	450	500	600	700
Capacity (VAh)	4560	5760	8640	11520	14400	20160
Maximum Depth of Cut (cm)	4	5	6	7	8	8
Width of the blade (m)	1.25	1.25	1.25	1.25	1.25	1.5
Blade Capacity (m³ loose)	0.15	0.15	0.20	0.26	0.33	0.45
Cost ($) without sensors	2500	4600	6300	8050	9800	12500

Table 2. Assigned parameters throughout the simulation

Symbol	Explanation	Value	Unit
v_e	Empty velocity	1.5	m/s
v_h	Hauling velocity	1.0	m/s
v_{ex}	Excavating velocity	0.75	m/s
μ	Friction coefficient between the hauled material and the ground surface	0.25	-
γ	Density of loose soil	12.000	N/m³
c	Cohesion of soil	24.000	N/m²
c_a	Soil to metal adhesion	12.000	N/m²
δ	Angle of soil to metal friction angle	40	Degree
α	Rake angle	55	Degree
η_m	Efficiency of electric motors	0.80	-
η_a	Efficiency of accumulators	0.87	-
k_s	Swell factor	1.3	-
φ	Angle of internal shearing resistance of the soil	30	Degree
P_e	Tire penetration of empty movement state	0.01	m
P_g	Tire penetration of hauling and grading states	0.03	m

the manufactured dozer. The simulation also aims to estimate the expected cost and the duration of the earthwork if more powerful dozers are utilized. The manufacturing costs of the dozers are estimated by conducting a market survey on the prices of accumulators, electric motors, and control circuits. The blade capacity and the depth of cut are determined based on the excavation velocity, power of the motors, and the weight of the machine. The cost of manufacturing of the body of the dozer is estimated by using the ratio of the body weight to electric motor power of the existing dozer.

Velocities of dozer given for different cases in Table 2 are the measured velocities of the manufactured small scale dozer. The soil parameters are derived by literature review [19-24]. Efficiencies of the electric motors and accumulators are the average values obtained from the data sheets of the market products.

The data about the graded zone and the related parameters are given in Table 2. Dimension of the excavated area

is 30 by 45 meters. Spatial resolution of the DEM is 1 meter. The elevation model is converted to 1.25x1.25 grids for the first five simulations and 1.5x1.5 grids for the sixth simulation. The ground surface is excavated until 960 meter which makes 1692.88 m³ of excavation. The results of the simulation are illustrated in Table 3.

The simulation time column illustrates the computation duration of the simulations. The duration column represents the duration of the excavation in terms of work hours. The energy column represents the consumed energy computed by considering the efficiencies of the motors and the accumulators. The fixed cost is computed by assuming that the construction machine will have 16.000 work hours of service life. This makes the hourly fixed cost equal to the 0.000171 times of the purchase price of the construction machine according to the unit price analysis of the Republic of Türkiye Ministry of Environment, Urbanization and Climate Change. The operator cost is not included since the construction machines are autonomous. The costs of

Table 3. Results of the simulation

	Simulation Time (sec)	Duration (h)	Energy (kWh)	Fixed Cost ($)	Energy Cost ($)	Total Cost ($)	Unit Cost ($/m³)
D1	23.96	152.76	108.92	65.30	14.16	79.46	0.047
D2	23.81	152.00	93.98	119.56	12.22	131.78	0.078
D3	17.99	113.70	88.52	122.49	11.51	134.00	0.079
D4	14.08	88.80	87.92	122.24	11.43	133.67	0.079
D5	13.06	77.28	80.34	129.51	10.44	139.95	0.083
D6	10.08	54.56	78.32	116.63	10.18	126.81	0.075

the construction machines given in Table 1 are multiplied by the duration and the hourly fixed cost coefficient and the figures given under the fixed cost column are obtained. The unit energy price is taken as 0.13$/kWh and the energy cost is obtained by multiplying the consumed energy with the unit energy cost. Total cost is the summation of the fixed cost and the energy costs. The unit cost is obtained by dividing the total cost by the total excavation amount. The soil type of the simulated excavation is soft soil whose unit price is 0.40$/m³ according to the unit price analysis of the Republic of Türkiye Ministry of Environment, Urbanization and Climate Change.

The simulation reveals that D1 consumes the highest energy and D6 consumes the least energy while executing the same grading task. D6 is more powerful and executes the grading with fewer passes. D1 consumes more energy while shuttling along the local highest point and the dump area. D1 provides the least unit excavation cost because it has the least fixed cost due to cheap lead-acid power supply. The simulated earthwork task is also examined by diesel powered Caterpillar D8 dozer which is a medium sized dozer. The rated power of the engine is 226 kW, the operating weight is 37557 kg with 8.7 m³ blade capacity. The duration computations are conducted according to the output computation charts provided by Caterpillar Company [38]. The simulation algorithm is not implemented for the Caterpillar D8 dozer since the aforementioned dozer can perform uphill dozing for the examined soil conditions. This shortens the total path of the dozer thus reduces the duration of the earthwork. The excavation is expected to be completed within 6 hours by Caterpillar D8 dozer. The simulation results illustrate that the electric powered dozers are slow but cost efficient construction machines. The unit excavation costs of all electric powered dozers are less than diesel dozers because the efficiency of the internal combustion engines is lower than the electric motors.

DISCUSSION OF RESULTS

In this study, simulation of an autonomous grading algorithm is performed on a small fictitious region. The simulation represent that the forces acting on the dozer can be computed for any movement of the dozer without any numerical problem. This ensures that the proposed autonomous grading algorithm and the formed force model are applicable. The formed force model contains some simplifying assumptions in order to decrease the complexity and the computational demand. The frictional losses due to the deflection of the tires and penetration of tires to the ground are computed by very simple formulas. On the other hand, the aforementioned equations are commonly used for the output calculations of the construction machines.

The dozer specifications from D1 to D6 are formed by considering at least two hours of working without charging. The mentioned work duration is adopted in order to fairly compare the investment and the unit excavation costs. The

simulation can be modified in order to examine the effects of longer recharge period. However, two hours of work period is inadequate and the usage of electric powered construction machines can become widespread if the prices of the lithium-ion batteries reduce.

The developed model and the simulation technique can be beneficial for the construction machine producers to estimate the operational costs of their products. Cost optimization analysis can be conducted to determine the optimum blade capacity, rimpull, cutting depth and cutting velocity. Different design alternatives can be analyzed in terms of target cost or operating cost and important competitive advantage can be obtained. Moreover, the simulation technique can be beneficial for the contractors as well, since they can predict the cost and duration of the earthwork very accurately. The contractor can examine several available dozer choices and can take the correct decision by considering the estimated costs and duration alternatives. The proposed simulation technique can be beneficial for both the construction machine producers and the contractors.

The simplifying assumptions of the simulation process can be listed as constant ground elevation for the grid size, no spill out of soil from the earth pile, constant acceleration throughout the velocity changes, constant surcharge pressure of the earth pile, and constant soil parameters throughout the excavation area. The effects of the aforementioned simplifications on the simulation results are discussed.

Constant ground elevation through the grid cell affects the cutting force because the real surface would be non-uniform and the depth of cut will fluctuate. This would cause anomalies such as instantaneous inadequate rimpull, rotational moment on the dozer, fluctuations of the velocity and power consumption of the dozer. On the other hand, amount of total excavation is not affected since the elevations of the grid cells are computed by bilinear interpolation from a DEM. Constant elevation assumption is necessary because spatial resolutions of commercial DEM products are significantly coarser than the implemented spatial resolution. Superior techniques to the current state-of-the-art DEM generation techniques should be implemented in order to obtain sufficient spatial resolution. Therefore the constant ground elevation for the grid size assumption is reasonable when the accuracies of the state-of-the art georeferencing methods are considered [39].

The spill out rate depends on the height of the earth pile, shape of the blade and the depth of the excavated slot in which the dozer moves. Volume of the earth pile is small because of the limited rimpull of the dozers. There is not any spill out from the manufactured dozer, because the volume of the earth pile is small. The simulated fictitious dozers have slightly bigger earth pile capacity. Therefore, important amount of spill out from the sides of the blade is not expected when the fictitious dozers are considered. In real case the volume of the spill out and the volume of the excavated soil become in an equilibrium state in which the
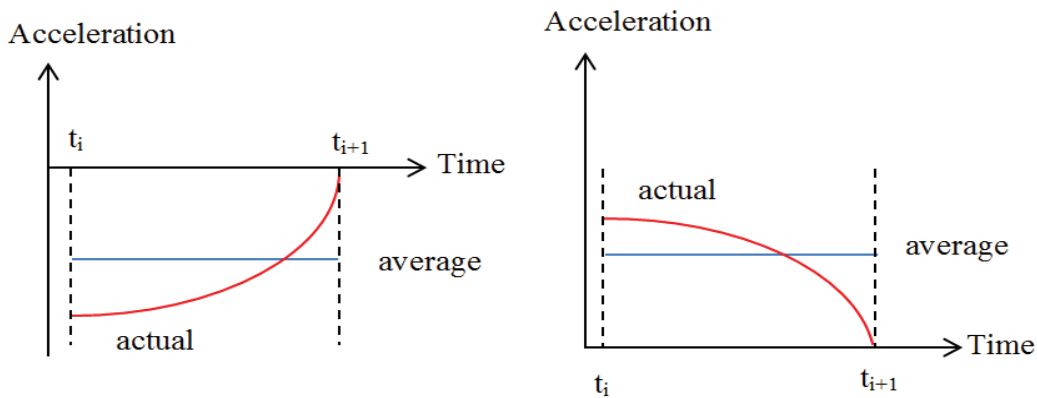
Figure 8. Illustration of the error of constant acceleration assumption.

dozer excavates a very thin portion of the ground and the same volume of the earth spills out so that the volume of the earth pile remains constant. The dozer excavates a certain portion of earth when it moves if the inflow and the outflow of earth is the same. The same volume of earth is spilled out from the blade and the amount of the earth pile in front of the blade does not change. This phenomenon is considered by Xia superficially, without taking the soil conditions, and the depth of the slot into account. In order to generate a realistic model, experimental studies should be conducted. Smaller mesh size should be assigned to model the height difference between the earth pile and the ground surface accurately. However, decreasing the mesh size will increase the computation time of the simulation.

Acceleration of the dozer is assumed to be constant when the state of the dozer shifts from excavation to hauling or empty movement vice versa. The magnitude of the acceleration is maximum in the beginning and it is zero when the maneuver is completed. The mentioned assumption deteriorates the estimations of the excavation time and the consumed energy.

In real situation, the acceleration of the dozer is expected to be higher in absolute value at the beginning of the state change of the dozer as shown in Figure 8a and 8b. The traction force exerted by the dozer is not adequate to preserve the velocity of empty state when it starts the excavation. The difference between the required force and the available force will be large and the dozer will have negative acceleration as shown in Figure 8a. The velocity of the dozer will reduce and the gap between the required force and the available force will decrease since the velocity of the dozer decreases and the power of the dozer divided by the velocity of the dozer will provide a larger traction force. The mesh size of the simulation is small enough to keep the time interval at most 2 seconds. However, in order to improve the accuracy of the simulation a quadratic acceleration model can be implemented as a future research.

The surcharge load due to the weight of the earth pile is assumed to be uniformly distributed which is not the case.

The highest point of the earth pile is slightly in front of the dozer blade and it decreases with the distance from the dozer blade. The adopted surcharge load model does not take the effect of the parabolic surcharge load. Therefore, uniform earth pile distribution is reasonable. The effect of non-uniform surcharge loading should be examined by in situ experiments. The soil parameters are assumed to be constant throughout the excavation area. Contractors which execute earthwork such as grading a garden of a school etc. can implement the developed autonomous grading algorithm. However, the developed algorithm is not suitable for earthwork tasks covering large region such as highway or airport construction. In order to take the variations of soil parameters into account, the simulation model should be Geographical Information System (GIS) based in which the soil data is associated with the spatial coordinates. This can be executed as a future research. Moreover, when the depth of excavation increases it is expected that the density, cohesion and internal friction angle of the soil also increase. In this study, the depth of excavation is around 1.5 meters which would not have a significant effect on the soil parameters. Effect of depth of excavation should be taken into account for deep excavations. The dozer blade interacts with the ground surface and disturbs the top soil which will reduce the cutting resistance. The aforementioned simplifications can be removed by implementing discrete element model analysis as future study.

The capacities of lead-acid batteries are limited while the lithium-ion batteries are expensive. However, the dozer with lead-acid battery will be too heavy to move if it is assembled with enough capacity to work for a long duration. The simulation revealed that the dozer with lead-acid power supply has the minimum unit excavation cost. However, lead-acid battery with the same capacity is significantly heavier and occupies more space than lithium-ion batteries. Therefore lead-acid batteries are not appropriate for a day long uninterrupted operation.

The grading algorithm prevents uphill dozing because of the inadequate rimpull of the electric powered dozer. If

a robust spill out model can be formed, some of the soil hauled in front of the blade can be spilled out by rotating the blade in case of an inadequate rimpull while uphill dozing. This will enable uphill dozing and the autonomous dozing algorithm can be enhanced.

CONCLUSION

In this study, the proposed autonomous grading algorithm is simulated on the small scale electric powered dozers. The simulation is executed on existing D1 and five fictitious D2 to D6 dozers. The simulation considers rolling, tire penetration, grade, hauling, as well as cutting resistances and computes the necessary power of the dozer to be supplied via its electric motors. The simulations are executed for different depth of cut, blade width, and rimpull without any numerical error. The simulations reveal that the electric powered dozers have less unit excavation costs than diesel powered dozers. In addition to this, if the rimpull of the dozer increases, number of the required passes reduces and this reduces the consumed energy and duration to execute the earthwork. Dozers with lithium-ion batteries have high investment and operating costs which are computed according to the unit price analysis of the Republic of Türkiye Ministry of Environment, Urbanization and Climate Change. The cost of grading and pushing the excavated material at most 20 meters away is computed as less than 5 cents/m^3 for the lead-acid battery powered dozer and 8 cents/m^3 in the average for the lithium-ion battery powered dozers. The smallest dozer D1 has 11.08 m^3/hour output and the largest dozer has 31.03 m^3/hour output.

The force model of the simulation has some simplifying assumptions to lessen the computational complexity and burden so that the computations of the simulation are executed within reasonable time. The simulation process can be beneficial for construction machine manufacturers to minimize the unit excavation cost of the dozer and optimize the capacity of the designed electric powered dozer. The contractors can examine the available dozers in the market and obtain their cost and duration of the earthwork task. The contactor can make a time-cost trade-off analysis and choose the most suitable dozer. Consequently, this study can be beneficial for both construction machine manufacturers and contractors.

ACKNOWLEDGMENT

DECLARATION OF ETHICAL STANDARDS

The author declares that the conducted study does not require any ethical permission.

AUTHORS' CONTRIBUTIONS

Önder Halis BETTEMİR: Developed the autonomous grading simulation algorithm and write the computer codes.

CONFLICT OF INTEREST

There is no conflict of interest in this study.

REFERENCES

[1] Zhong D, Ping Z, KangXin W. Theory and practice of construction simulation for high rockfill dam. Sci China Technol Sci 2007;50:51−61. [CrossRef]

[2] Lu M, Chen W, Shen X, Lam HC, Liu J. Positioning and tracking construction vehicles in highly dense urban areas and building construction site. Autom Constr 2007;16:647−656. [CrossRef]

[3] Vahdatikhaki F, Hammad A, Siddiqui H. Optimization-based excavator pose estimation using real-time location systems. Autom Constr 2015;56:76−92. [CrossRef]

[4] Hammad A, Vahdatikhaki F Zhang C. A novel integrated approach to project-level automated machine control/guidance systems in construction projects. J Inf Technol in Constr 2013;18:162−181.

[5] Jurasz J, Kley K. A Cost-effective positioning solution for asphalt rollers based on low-cost DGPS receivers. In proceedings of the 19th International Symposium on Automation and Robotics in Construction; 2002 Sept 23-25; Washington, USA. 2002. p. 403−408. [CrossRef]

[6] Hung WH, Kang SCJ. Automatic clustering method for real-time construction simulation. Adv Eng Inform 2014:28:138−152. [CrossRef]

[7] Oloufa A, Ikeda M, Oda H. Situational awareness of construction equipment using GPS, wireless and web technologies. Autom Constr 2003;12:737−748. [CrossRef]

[8] Oloufa A, Ikeda M, Oda H. GPS-based wireless collision detection of construction equipment. 19th International Symposium on Automation and Robotics in Construction; 2002 Sept 23-25; Washington, USA. 2002. p. 461−466. [CrossRef]

[9] Hammad A, Vahdatikhaki F, Zhang C, Mawlana M, Doriani A. Towards the smart construction site: Improving productivity and safety of construction projects using multi-agent systems, real-time simulation and automated machine control. In proceedings of the IEEE Proceedings of the 2012 Winter Simulation Conference (WSC); 2012 Dec 1-12; Berlin, Germany. IEEE; 2012. [CrossRef]

[10] ElNimr A, Fagiar M, Mohamed Y. Two-way integration of 3D visualization and discrete event simulation for modeling mobile crane movement under dynamically changing site layout. Autom Constr 2016;68:235−248. [CrossRef]

[11] Vahdatikhaki F, Hammad A. Risk-based look-ahead workspace generation for earthwork equipment using near real-time simulation. Autom Constr 2015;58:207−220. [CrossRef]

[12] Blackmore BS, Griepentrog HW. Autonomous Vehicles and Robots. In: Munac A, editor. CIGR handbook of agricultural engineering. Michigan, USA: ASABE; 2006. p. 204−215.

[13] Murad Ç, Yıldız E. Sera Üretim Mekanizasyonunda Robotik Uygulamalar: Literatür Çalışması. In: Marakoğlu T, editor. Proceedings of the 28. Ulusal Tarımsal Mekanizasyon Kongresi; 2013 Sept 4-6; Konya, Türkiye. Aybil Yayınları; 2013. p. 269−281.

[14] Kılıç A, Kapucu S. Modüler yeniden yapılandırılabilir robot modülü OMNIMO'nun tasarımı ve üretimi. J Fac Eng Archit Gazi Univ 2016;31:521−530. [CrossRef]

[15] Bettemir Ö, Tombaloglu B. Küçük ölçekli otonom iş makinesi tasarımı ve üretimi. J Fac Eng Archit Gazi Univ 2013;28:617−625.

[16] Yıldırım A, Bettemir ÖH. Otonom dozer için küreme algoritması geliştirilmesi. Düzce Üniv Bil Teknol Derg 2018;6:292−308. [CrossRef]

[17] Bettemir ÖH. Otonom iş makinesinde çoklu CP DGPS kullanımı etkisinin benzetim ile tayini. In proceedings of the 2013 Otomatik Kontrol Ulusal Toplantısı; 2013 Sept 26-28; Malatya, Türkiye. 2013. p. 733−737.

[18] Bettemir ÖH. Development of mini scale autonomous robot grader for road constructions. In proceedings of the International Workshop on Unmanned Vehicles; 2010 Jun 10-12; İstanbul, Türkiye. 2010. p. 1−16.

[19] Fall A, Weber B, Pakpour M, Lenoir N, Shahidzadeh N, Fiscina J, et al. Sliding friction on wet and dry sand. Phys Rev Lett 2014;112;175502. [CrossRef]

[20] Klanfar M, Kujundžić T, Vrkljan D. Calculation analysis of bulldozer's productivity in gravitational transport on open pits. Teh Vjesn 2014;21:517−523.

[21] Patel BP, Prajapati JM, Gadhvi BJ. An excavation force calculations and applications: An analytical approach. Int J Eng Sci Technol 2011;3:3831−3837.

[22] McKyes E, Ali OS. The cutting of soil by narrow blades. J Terramech 1977;14:43−58. [CrossRef]

[23] Zeng X, Burnoski L, Agui J, Wilkinson A. Calculation of excavation force for ISRU on lunar surface. Available at: https://ntrs.nasa.gov/api/citations/20070018151/downloads/20070018151.pdf. Accessed on May 15, 2024.

[24] Xia K. A framework for earthmoving blade/soil model development. J Terramech 2008;45:147−165. [CrossRef]

[25] Yıldırım A, Bettemir ÖH. Visualisation of grading simulation. In Proceedings of the International Civil Engineering & Architecture Conference; 2019 Apr 17 - 20; Trabzon, Turkey. 2019.

[26] Nunnally SW. Construction Methods and Management. 6th edition. McGraw-Hill, USA: Prentice Hall; 2003.

[27] Holz D, Azimi A, Teichmann M, Mercier S. Real-time simulation of mining and earthmoving operations: a level set-based model for tool-induced terrain deformations. In Proceedings of the International Symposium on Automation and Robotics in Construction; 2013 Aug 11-15; Montreal, Canada. Curran Associates; 2013. p. 468−477. [CrossRef]

[28] Reece AR. The fundamental equation of earthmoving mechanics. In proceedings of 1964 Institution of Mechanical Engineers Conference; 1964 Jun 1.

[29] Kato, K. Wear in relation to friction - A review. Wear 2000;241:151−157. [CrossRef]

[30] Hoornaert T, Hua ZK, Zhang JH. Hard Wear-Resistant Coatings: A Review. In: Luo J, Meng Y, Shao T, Zhao Q, editors. Advanced Tribolgy. Heidelberg, Berlin: Springer; 2009. p. 774−779. [CrossRef]

[31] Duarte I, Ferreira JMF. Composite and nanocomposite metal foams. Materials (Basel) 2016;9:79. [CrossRef]

[32] Bolat Ç, Akgün İC, Gökşenli A. Effects of particle size, bimodality and heat treatment on mechanical properties of pumice reinforced aluminum syntactic foams produced by cold chamber die casting. China Foundry 2021;18:529−540. [CrossRef]

[33] Ergene B, Bolat Ç. Determination of thermal stress and elongation on different ceramic coated Ti-6Al-4V alloy at elevated temperatures by finite element method. Sigma J Eng Nat Sci 2020;38:2013−2026.

[34] Steffensen JF. Interpolation. 2nd ed. Mineola, NY: Courier Corporation; 2006.

[35] Shi WZ, Li QQ, Zhu CQ. Estimating the propagation error of DEM from higher-order interpolation algorithms. Int J Remote Sens 2005;26:3069−3084. [CrossRef]

[36] Perissin D, Rocca F. High-accuracy urban DEM using permanent scatterers. IEEE Trans Geosci Remote Sens 2006;44:3338−3347. [CrossRef]

[37] Caterpillar, 1979. Fundamentals of Earthmoving. Texas, US: Caterpillar Tractor Company; 1963.

[38] Bettemir ÖH. Prediction of georeferencing precision of pushbroom scanner images. IEEE Trans Geosci Remote Sens 2011;50:831−838. [CrossRef]